Image Enhancement and Quality Measures for Dietary Assessment Using Mobile Devices

Chang Xu,[a] Fengqing Zhu,[a] Nitin Khanna,[a] Carol J. Boushey,[b,c] and Edward J. Delp[a]

[a]School of Electrical and Computer Engineering and [b]Department of Nutrition Science
Purdue University, West Lafayette, Indiana, USA
[c]Epidemiology Program, University of Hawaii Cancer Center
Honolulu, Hawaii, USA

ABSTRACT

Measuring accurate dietary intake is considered to be an open research problem in the nutrition and health fields. We are developing a system, known as the mobile device food record (mdFR), to automatically identify and quantify foods and beverages consumed based on analyzing meal images captured with a mobile device. The mdFR makes use of a fiducial marker and other contextual information to calibrate the imaging system so that accurate amounts of food can be estimated from the scene. Food identification is a difficult problem since foods can dramatically vary in appearance. Such variations may arise not only from non-rigid deformations and intra-class variability in shape, texture, color and other visual properties, but also from changes in illumination and viewpoint. To address the color consistency problem, this paper describes illumination quality assessment methods implemented on a mobile device and three post color correction methods.

Keywords: dietary assessment, mobile devices, color correction, quality measure

1. INTRODUCTION

There is a growing concern with respect to chronic diseases and other health problems related to diet including obesity and cancer. Dietary intake, the process of determining what someone eats during the course of a day, provides valuable insights for mounting intervention programs for prevention of many chronic diseases. Measuring accurate dietary intake is considered to be an open research problem in the nutrition and health fields[1, 2].

Mobile telephones can provide a unique mechanism for collecting dietary information that reduces the burden on record keepers. A dietary assessment application that uses a mobile telephone for collecting information would be of value to practicing dietitians and researchers[3, 4]. Previous results among adolescents showed that dietary assessment methods using a technology-based approach, e.g., a personal digital assistant with or without a camera or a disposable camera, were preferred over the traditional paper food record[3]. This suggests that for adolescents, dietary methods that incorporate new mobile technology may translate to improved cooperation and accuracy.

We described in[5] a mobile device food record (mdFR) that the team at Purdue University and the University of Hawaii Cancer Center developed using a mobile device (e.g. a mobile telephone or PDA-like device) to provide an accurate account of daily food and nutrient intake. Our goal is to use the mobile device with a built-in camera to allow a user to discretely record foods eaten. Each food item in the image is segmented, identified, and its volume is estimated[5–7]. Images acquired before and after foods are eaten can be used to estimate the food intake.

This system is known as the Technology Assisted Dietary Assessment System or the TADA System[5]. The TADA system consists of two main parts: a mobile application we refer to as the mobile device food record (mdFR) and the "backend" system consisting of the compute server and database system. Figure 1 shows the overall architecture of our proposed system. The first step is to send the image acquired with the mobile telephone and metadata to the server for automatic analysis, including image segmentation, food identification and volume estimation (steps 2 and 3). These results are sent back to the user where the user confirms and/or adjusts this information (step 4). In step 5, the server receives the confirmed information from the user. Based on the user feedback, refinements are done to the image segmentation and

This work was sponsored by grants from the National Institutes of Health under grants NIDDK 1R01DK073711-01A1 and NCI 1U01CA130784-01. Address all correspondence to E. J. Delp: ace@ecn.purdue.edu

Computational Imaging X, edited by Charles A. Bouman, Ilya Pollak,
Patrick J. Wolfe, Proc. of SPIE-IS&T Electronic Imaging, SPIE Vol. 8296, 82960Q
 · doi: 10.1117/12.909949

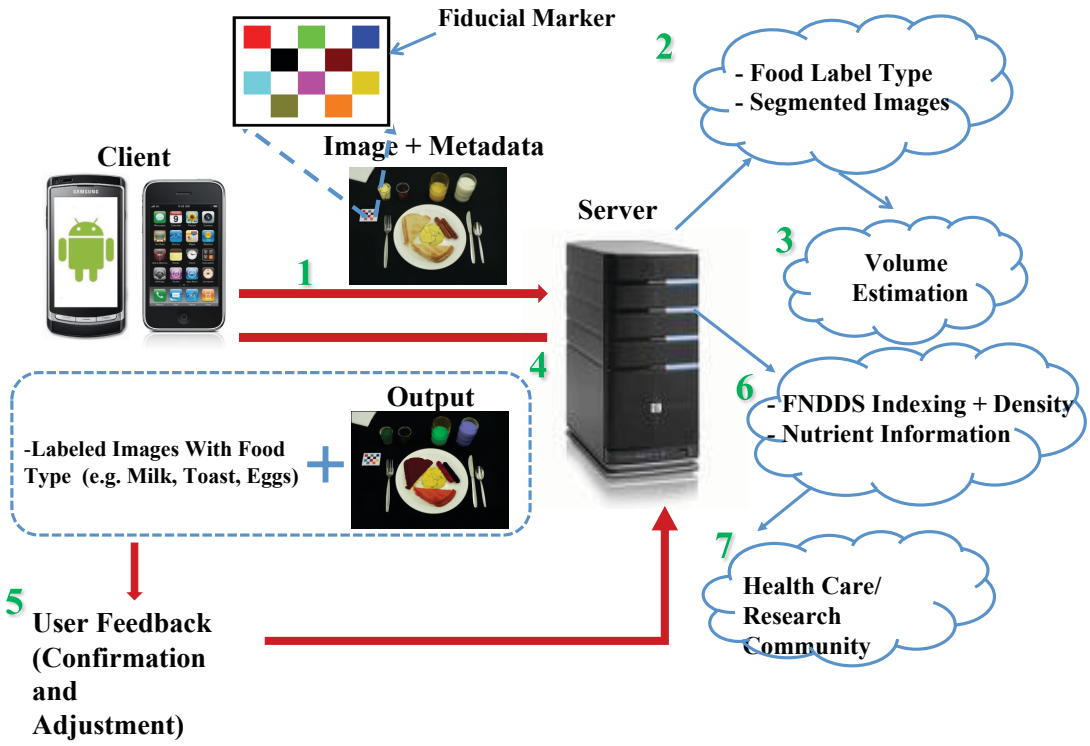

Figure 1. The Architecture of the TADA System.

food labeling. Nutrient information is extracted using the USDA Food and Nutrient Database for Dietary Studies (FNDDS) database[8] complemented with density data. FNDDS is a database containing foods eaten in the U.S., their nutrient values, and weights for different standardized food portions (step 6). Finally these results can be sent to the research community for further analysis (step 7). We have deployed this system on an Apple iPhone and it is currently being validated in the Department of Nutrition Science at Purdue University and the University of Hawaii Cancer Center among adolescents and adults.

Since we are interested in knowing how much food is consumed, we need to have a 3D calibrated imaging system. In the current version of the TADA system a user takes only one image of the food and 3D models are used to construct the 3D object[7]. Other approaches include acquiring multiple images of the food scene from different "views." The methods used for constructing the 3D information is beyond the scope of this paper. Whatever approach is used, we still have to have a calibrated imaging system that is calibrated both spatially and with respect to the colors represented in the scene. This can be accomplished by having the user acquire the image with a known object, e.g., a pen or PDA stylus, placed next to the food so one could use this to calibrate sizes in the image. One might also use the known dimensions of a plate or cup in a scene. Other a priori information in the scene such as the pattern on the tablecloth could also be used. We have chosen to use a checkerboard-like design as a particular type of "fiducial marker" for our calibration information. The fiducial marker is included in every image to provide a reference for the scale and pose of the objects in the scene and to provide color calibration information. After testing several designs, we decided to use a compact checkerboard pattern (see Figure 1). Several studies conducted by the Department of Nutrition Science at Purdue University asked participants to take images of their food before and after meals[4, 9]. Responses from the participants in these studies indicated that it would be easy to use a credit card-sized fiducial marker due to the convenient incorporation into their current lifestyles.

Through experimentation, the best properties of the checkerboard have been determined as follows: the pattern is an asymmetric checkerboard with [odd] $\times$ [even] dimensions, minimum 4 tiles per side, high contrast, matte finish, and rigid mounting. In our studies, it is a small (7×6 cm^2) colored checkerboard (see Figure 2). Lighting conditions and camera quality can affect the appearance of color in the acquired images. Since the recognition of food relies heavily on color features, it is important to incorporate color information into the design. We need to detect the fiducial marker in the scene

so that we can use the calibration information. This is done using only the gray scale version of the image acquired from the camera. Since we use the color fiducial marker to also calibrate the color information in the scene, the gray scale image of the color marker has somewhat less contrast than a true black and white fiducial marker and can affect our ability to recognize the corners. Therefore we must take this into account when designing the color fiducial marker.

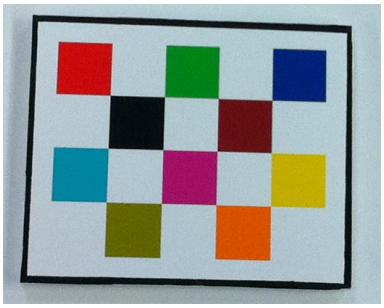

Figure 2. An Example of the Color Fiducial Marker Used in the TADA System.

Full utilization of the side information provided by the use of a fiducial marker and other contextual information is very important for dealing with the challenges involved in food classification and volume estimation from a single image. For example, food identification is a difficult problem since foods can dramatically vary in appearance[5]. Such variations may arise not only from non-rigid deformations, and intraclass variability in shape, texture, color and other visual properties, but also from changes in illumination and viewpoint. Color features play a very important role in food identification. Many food items have closely related colors under a wide range of illumination conditions. Thus, color correction plays a crucial role in dietary assessment methods[5, 10]. Most of these methods use some sort of fiducial marker for estimating unknown illumination conditions and subsequently use color correction methods for mapping the test image back to the reference illumination conditions. Similarly, the fiducial marker plays a key role in 3D reconstruction from 2D images for estimating the volumes of different food items[7, 10]. Hence, integrating a real-time image color quality check on the mobile device will result both in a better user experience with lesser user burden and in circumventing image analysis problems due to images of inadequate quality.

This paper describes image color quality assessment methods using the mobile device and post processing for color correction. Our goal is to detect image quality problems before users "save" images of their meals and assist them with capturing better images. Apart from the general notion of image quality such as sharpness, in the context of dietary assessment, good quality images need to satisfy specific requirements such as the presence of the fiducial marker and appropriate camera pose. Based on our user studies the most significant reasons for poor quality images are: failure to detect the presence of the fiducial marker (forgetting to use the fiducial marker or overexposed/blurred images), spectral reflections, shadows, insufficient illumination, and blur.

While some of the correction steps can be done on the mobile device, computationally intensive steps including color correction are done on the server. Doing all the image quality assessment on the server and then sending back the response to the user is not feasible in most circumstances, due to associated network and computation delays. Mobile devices have limited computation power and some of the image quality check needs to be performed before the image is saved. We have found that a quick illumination check can be implemented on the mobile device without adding any perceptible delay in the image capture.

2. OVERVIEW OF COLOR CORRECTION

Color can serve as one of the key variables in imaging[11]. A consistent color descriptor of an object is very useful to improve the results of image analysis. The colors of objects recorded by camera depend on three factors. First, illumination conditions in the scene are unknown in most circumstances. Second, objects in the scene have different intrinsic surface properties which produces spectral reflection given the light conditions. Moreover, the capturing device has various photometric parameters (e.g., exposure time, white balancing, gamma correction) that affect the color representation

of the objects in a scene. Therefore how one can increase the robustness of the color descriptor remains one of the major challenges for current color imaging systems.

Some approaches seek to overcome these problems by estimating illumination invariance color descriptors from a database of images. These features include the RGB histogram, color moments, and C-SIFT[12–14]. In[12], a combined set of color descriptors with invariance properties surpass the performance of intensity based descriptors by 8% on category recognition.

Another approach to deal with this issue is to estimate the intrinsic relationship between images illuminated with reference lighting and images acquired with unknown lighting conditions. In this approach, color correction is often used for determining perceptual consistency. By using this process, the overall color characteristics of the image will be improved, and at the same time, color differences under low light conditions will be enhanced, which can also be beneficial to image segmentation.

Color correction, also known as *color balancing* is the global adjustment of the color intensities in an image. The goal of such adjustment is to render neutral colors in an image correctly. Color correction changes the overall colors in an image and is often used for colors other than neutrals to appear correct or pleasing. Methods for this type of correction are generally known as gray balance, neutral balance or white balance [15]. There are many color correction methods [16–18]. In general, most of these methods contains two steps: first, estimate the illumination color temperature of the scene by using the image data and statistical information. Then, use the illumination parameters to obtain the color corrected image. However, in our application, we not only have the illumination parameters which are estimated from the white patch on the fiducial marker, we also have the other color information from all 11 color patches on the fiducial marker. Our goal is to improve the overall color correction accuracy using all the information from the fiducial marker.

In an earlier approach we used the color correction method described in[19]. This approach represented illumination color features using the Macbeth color board with 24 colors. Conversion vectors were defined from a source illumination to a target illumination. Assuming that illumination A is the target, a conversion vector from illumination B to illumination A can be defined for each color patch on the Macbeth color board. For each color path i, the conversion vector C_i is defined as the difference between RGB color of each path in illuminations A and B. Thus, the conversion vector from illumination B to illumination A, C_{A-B}, is an average vector of conversion vectors of all color patches, equivalently,

$$C_{A-B} = \frac{1}{24}\sum_{i=1}^{24} C_i = (C_r, C_g, C_b) \tag{1}$$

The illumination conversion vector is then used according to the pixel color in images of illumination B. Let the RGB value of a pixel at (x, y) in the image of illumination B be (R_{xy}, G_{xy}, B_{xy}). This color value (R_{xy}, G_{xy}, B_{xy}) is corrected by adding the illumination conversion vector C_{A-B} above as follows

$$\left(R_{xy}^{'}, G_{xy}^{'}, B_{xy}^{'}\right) = (R_{xy}, G_{xy}, B_{xy}) + (C_r, C_g, C_b) \tag{2}$$

We also adopted a simplified version of the approach proposed by Srivasrava, et al[20] to address the problem of visually matching two known display devices in color management systems. The method is implemented through the use of 3D look-up tables (LUT). In our case, we consider a uniformly sampled LUT of size $3 \times 3 \times 3$. Interpolation methods have been proposed in one and more dimensional spaces and on regular or irregular shaped data grids. In general cases, an input point $[x, y, z]_c$, whose output needs to be predicted, can have k neighbors $[x, y, z]_i$ for $i = 0, 1, ..., k-1$. Let $d(c, i)$ be some metric of distance between the points c and its neighbors i. Note that each neighbor is an entry in the table and hence their outputs $f([x, y, z])_i$ are known. Then using interpolation

$$f\left([x, y, z]\right)_c = \psi\left(f_i, d_i\right) \quad \text{for } i = 0, 1, ..., k-1 \tag{3}$$

where ψ is determined by the chosen method. For example, a simple 1D linear interpolation is

$$f_c = \left(f_0 \cdot d\left(c, 1\right) + f_1 \cdot d\left(c, 0\right)\right) / \left(d\left(c, 0\right) + d\left(c, 1\right)\right) \tag{4}$$

However, illumination change from the reference image to the target image is often not uniform in the RGB color space and the color appearance of the scene is a complex process affecting several things including camera behavior,

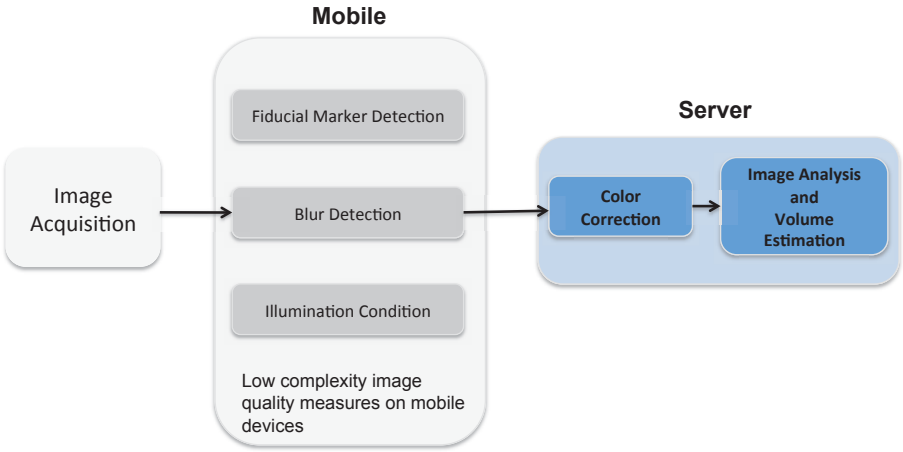

Figure 3. Our Proposed Quality Measure and Image Enhancement System.

the illumination condition and surface reflectance. Therefore a single conversion vector or 3D interpolation may not be sufficient to accurately correct colors in different regions in the image. To correct colors in an image containing the color fiducial marker from unknown sources or illuminations, we propose below three chromatic adaptation models that use more perceptually uniform color space models.

3. SCENE ILLUMINATION DETECTION USING COLOR MAPPING

Our methods begin with capturing an image of the color fiducial marker using a digital still camera or a mobile device camera under an unknown illumination and the use of known color patches on the fiducial marker as the reference colors. As shown in Figure 3, the next step is fiducial marker detection that will not be described here but is presented in[21]. After estimating 11 colors from the fiducial marker, we then evaluate the illumination condition by determining if the colors on the fiducial marker fall within a prescribed range of RGB values. The reason for performing the illumination check is to avoid bad illumination conditions, specifically too dark, too bright or wrong color temperature, and assist the user in capturing a better image before saving the image. Since the mobile device has limited computational power and memory resources, the color correction step is performed on the server (see Figure 1).

The RGB components of the color patches on the fiducial marker from the acquired image are extracted and mapping between the reference fiducial marker colors and the colors from the fiducial marker from the acquired image are established[22]. Finally, this mapping is used to correct the colors of the acquired image to match the reference colors. We investigated three different color correction methods: a linear RGB to RGB transform, a nonlinear RGB to RGB transform, and a linear model in LAB color space.

3.1. Color Space Models

First, a linear RGB mapping color correction method based on the von-Kries model[23] is introduced. A chromatic adaptation transformation (CAT) mapping XYZ_1 in viewing condition 1 to XYZ_2 in viewing condition 2 to achieve a perceptual match can be formulated as follows:

$$\begin{bmatrix} X_2 \\ Y_2 \\ Z_2 \end{bmatrix} = \boldsymbol{H}^{-1} \begin{bmatrix} \frac{L_{w2}}{L_{w1}} & 0 & 0 \\ 0 & \frac{M_{w2}}{M_{w1}} & 0 \\ 0 & 0 & \frac{S_{w2}}{S_{w1}} \end{bmatrix} \boldsymbol{H} \begin{bmatrix} X_1 \\ Y_1 \\ Z_1 \end{bmatrix}; \tag{5}$$

where LMS_{wi}, $(i = 1, 2)$, is the LMS cone responses to reference white w_i. $\boldsymbol{H}$ is a 3×3 non-singular matrix which represents a transformation from XYZ to LMS.

The transformation between RGB and CIE XYZ can be represented by a Bradford transform[24]:

$$\begin{bmatrix} R & G & B \end{bmatrix}^T = T_{3\times 3} \begin{bmatrix} X & Y & Z \end{bmatrix}^T \tag{6}$$

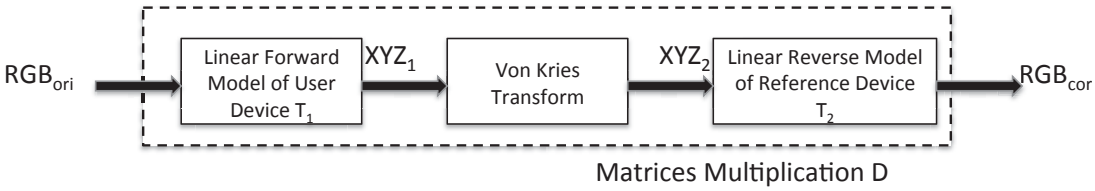

Figure 4. The Linear Model from RGB to XYZ.

where $T_{3\times3}$ is a forward transformation which is determined by the capturing device and illumination conditions.

We substitute Equation 5 into Equation 6. Then, we obtain a linear model which contains conversion matrix D in Figure 4 as follows:

$$\begin{bmatrix} R_{cor} \\ G_{cor} \\ B_{cor} \end{bmatrix} = \underbrace{\boldsymbol{T_2 H}^{-1} \begin{bmatrix} \frac{L_{w2}}{L_{w1}} & 0 & 0 \\ 0 & \frac{M_{w2}}{M_{w1}} & 0 \\ 0 & 0 & \frac{S_{w2}}{S_{w1}} \end{bmatrix} \boldsymbol{H T_1}^{-1}}_{\boldsymbol{D_{3\times3}}} \begin{bmatrix} R_{ori} \\ G_{ori} \\ B_{ori} \end{bmatrix}; \tag{7}$$

where R_{ori}, G_{ori} and B_{ori} is the RGB values of the original image and R_{cor}, G_{cor} and B_{cor} is the RGB values of the corrected image, respectively. The calibrated RGB value is simplified to the multiplication of the original RGB value with a 3×3 matrix D.

To determine the conversion matrix D, we formulate a least square regression problem that best transforms the 11 colors on the fiducial marker into corresponding reference colors:

$$D_{3\times3} = \arg\min_{D_{3\times3}} \sum_{i=1}^{11} \left\| (RGB_i)^t_{ref} - D_{3\times3} \, (RGB_i)^t_{ori} \right\|^2 \tag{8}$$

Where "ref" is the sRGB values of the 11 colors on the fiducial marker under the D65 illumination[22].

As described above, this method suggests a linear transformation between two RGB space images. However, this could lead to a over simplified system with low accuracy. We propose next a non-linear model with more color fidelity, where the color variation introduced by illumination conditions and camera models are considered.

In the previous model, we proposed a linear system based on the assumption that there is no interaction between each RGB channel. This assumption is not satisfied in many cases due to the factors including gamma correction, non-uniform illumination and image processing process integrated inside the camera. To account for these nonlinearities, we describe an approach for color correction using a non-linear 10×3 mapping between source image and target image. Let the vector $P_{10\times1}$ contain the cross product and second order terms of "R_{ref}", "G_{ref}" and "B_{ref}" described above:

$$P_{10\times1} = \begin{bmatrix} R_{ori} & G_{ori} & B_{ori} & R^2_{ori} & G^2_{ori} & B^2_{ori} & R_{ori}B_{ori} & R_{ori}G_{ori} & G_{ori}B_{ori} & 1 \end{bmatrix}^T \tag{9}$$

$$\begin{bmatrix} R_{cor} \\ G_{cor} \\ B_{cor} \end{bmatrix} = \boldsymbol{D}_{3\times10} P_{10\times1} \tag{10}$$

By using the 11 RGB values of the colors from our fiducial marker on the reference image and target image, the matrix D is formulated as an optimization problem.

$$D_{3\times10} = \arg\min_{D_{3\times10}} \sum_{i=1}^{11} \left\| (RGB_i)^t_{ref} - \boldsymbol{D}_{3\times10} P_{10\times11} \right\|^2 \tag{11}$$

Similarly to the last step of the linear model, the color correction image is obtained by multiplying the RGB value of the target image with 10×3 matrix D.

The last chromatic adaptation model we implemented is shown in Figure 5 and is based on the uniform CIELAB color space. Though both CIEXYZ and CIELAB are considered device-independent color spaces, the CIELAB color space includes all perceivable colors and is considered more perceptually uniform than CIEXYZ[25, 26]. Therefore, a linear mapping deployed in LAB color space might be more reasonable. A gamma correction is first used to obtain the linear

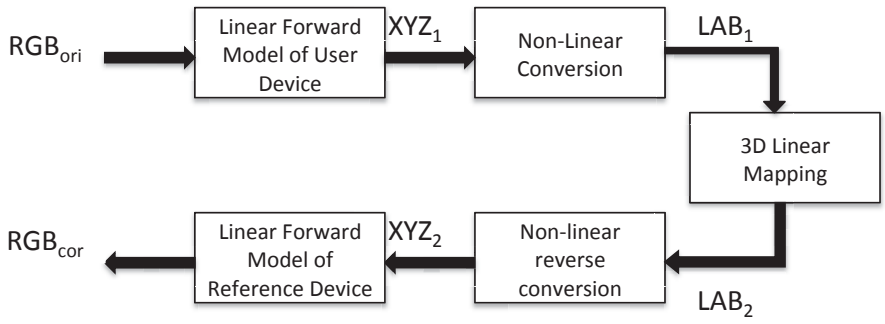

Figure 5. The Color Model from RGB to LAB.

RGB values. Based on the studies we have done we set the value of gamma to 1.1. After this, we map the original image from RGB to XYZ space with the Bradford Transform. The forward transformation matrix we are using is the sRGB standard with D65 illumination can be found in [27]. The following step is to normalize XYZ for the D65 white point. Finally, a non-linear forward transform between the normalized XYZ to LAB is obtained as follows[28]:

$$L = 116 * f(Y/Y_n) - 16 \tag{12}$$

$$a = 500 * [f(X/X_n) - f(Y/Y_n)] \tag{13}$$

$$b = 200 * [f(Y/Y_n) - f(Z/Z_n)] \tag{14}$$

$$f(x) = \begin{cases} (x)^{1/3} & \text{if } x > 0.008856 \\ 7.787(x) + 16/116 & \text{otherwise} \end{cases} \tag{15}$$

X_n, Y_n, and Z_n are the tristimulus values of the white point. The L coordinate in CIELAB is correlated to perceived lightness. The a and b coordinates are the red-green and yellow-blue of the color-opponent, respectively.

The transform in CIELAB space is perceptually uniform. We use a 3-dimensional linear transformation that converts the 11 LAB_1 values of the color patches from the fiducial marker in viewing condition 1 to the 11 LAB_2 values of the color patches in viewing condition 2. The 3×3 mapping matrix D is obtained as follows:

$$D_{3\times3} = \arg\min_{D_{3\times3}} \sum_{i=1}^{11} \left\| (LAB_i)_{ref}^t - D_{3\times3} \, (LAB_i)_1^t \right\|^2 \tag{16}$$

Finally, a reverse transform is done to convert the image from CIELAB to RGB.

Sample color correction results using these methods, as well as comparison to the methods described by Choi[19] and Srivastava[20] are described next in Section 4.

4. EXPERIMENTAL RESULTS

To evaluate the performance of our proposed color correction methods the following experiment was performed. Two test targets were used in the experiment, specifically the TADA color fiducial marker as shown in Figure 2 and a GretagMacbeth Colorchecker[29] which is a calibrated color reference chart. Both targets were placed inside a "SpectraLight II" illumination booth which provides four uniform calibrated light sources: simulated daylight (CIE D65, 6500 K), horizon daylight (simulated early morning sunrise or afternoon sunset, 2300 K), CIE A (incandescent home lighting, 2856 K),

and commercial fluorescent (cool white, 4000 K). Under each illumination an image of the targets was acquired using the camera on an iPhone 3GS.

The captured images under non-D65 illumination were then color corrected using the three methods described in the previous section as well as two other methods described by Choi[19] and Srivastava[20]. To evaluate the accuracy of each method, the euclidean distance between the average color of each color patch on the GretagMacbeth Colorchecker $\left(\widetilde{R}_i^t, \widetilde{G}_i^t, \widetilde{B}_i^t\right)$ and the known sRGB values of each patch under D65 illumination (R_i^r, G_i^r, B_i^r) (see Figure 6) was obtained using Equation 17 and are shown in Table 1. The euclidean distance is defined as:

$$\Delta = \frac{1}{24}\sum_{i=1}^{24}\left\|\left(\widetilde{R}_i^t, \widetilde{G}_i^t, \widetilde{B}_i^t\right)^t - (R_i^r, G_i^r, B_i^r)^t\right\| \tag{17}$$

Table 1. Mean RGB Channels Errors (Δ) Between the Reference Image and Transformed Images

Lighting	Error	Before	Linear-LAB	Linear-RGB	Polynomial	Srivastava	Choi
Horizon Light	RGB	37.20	16.13	25.47	26.26	33.91	34.04
	Red	14.87	7.18	9.36	8.30	13.20	9.81
	Green	7.57	3.88	5.16	5.22	6.54	12.93
	Blue	31.21	11.67	21.03	22.34	26.90	26.49
Incandescent	RGB	22.11	18.89	22.06	20.23	19.46	21.64
	Red	10.56	8.75	12.57	9.64	8.40	9.84
	Green	8.14	9.65	8.82	8.73	8.07	8.78
	Blue	14.84	10.34	13.39	13.59	13.14	13.64
Coolwhite	RGB	17.23	7.92	12.34	12.23	15.13	16.29
	Red	12.04	3.52	9.60	9.58	11.10	11.22
	Green	6.53	4.41	5.03	4.91	6.28	6.14
	Blue	6.74	3.97	3.69	3.61	4.47	5.72

Table 1 shows the mean RGB channels errors (Δ) between the reference image and transformed images for each method under three different illuminations, where each row shows the errors of all five methods under one lighting source, and each column shows the errors of one method under all three lighting sources. For example, the overall error of each method (Original, Linear-LAB, Linear-RGB, Polynomial, Srivastava and Choi) under the horizon lighting is 16.13, 25.47, 26.26, 33.91, 34.04 respectively.

From the results summarized in Table 1 and Figure 7, we can observe that our proposed methods usually have better color consistency in the various illumination tests than the methods derived by Choi[19] and Srivastava[20] in that the error, Δ, is smaller. Figure 7 shows the images after color correction.

The linear model in CIELAB color space has the best performance based on overall RGB error. When the white point is very different from D65 (i.e. Horizon light) it performs better than any other method. However, if we look at the individual color channels separately, it does not consistently have better correction. For example, the errors of the red and green channel under the incandescent light and the blue channel under the cool white light are 8.75, 9.65 and 3.97, which performs worse than some methods. This error could be introduced by the gamma correction step. Since we assume that we do not have any knowledge about the capturing device, the gamma value is fixed. The gamma value should be independent in each color channel and each device.

The linear model and the nonlinear model in RGB color space are better than the methods described by Choi[19] and Srivastava[20]. They both perform similarly and improve the overall color consistency. Nevertheless, we observed that these two methods introduce more error in the red and green channels under incandescent light. The reason for this error could be the simplified nature of our color appearance model.

5. CONCLUSION

In this paper we have presented three methods for illumination detection on a mobile device and several color correction methods. The proposed methods for color correction are deployed in the TADA system and are being tested under various

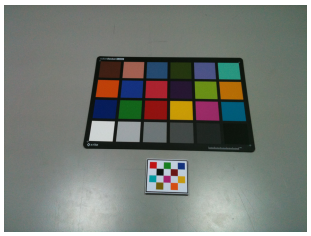

Figure 6. The Image With Reference Light Condition (D65).

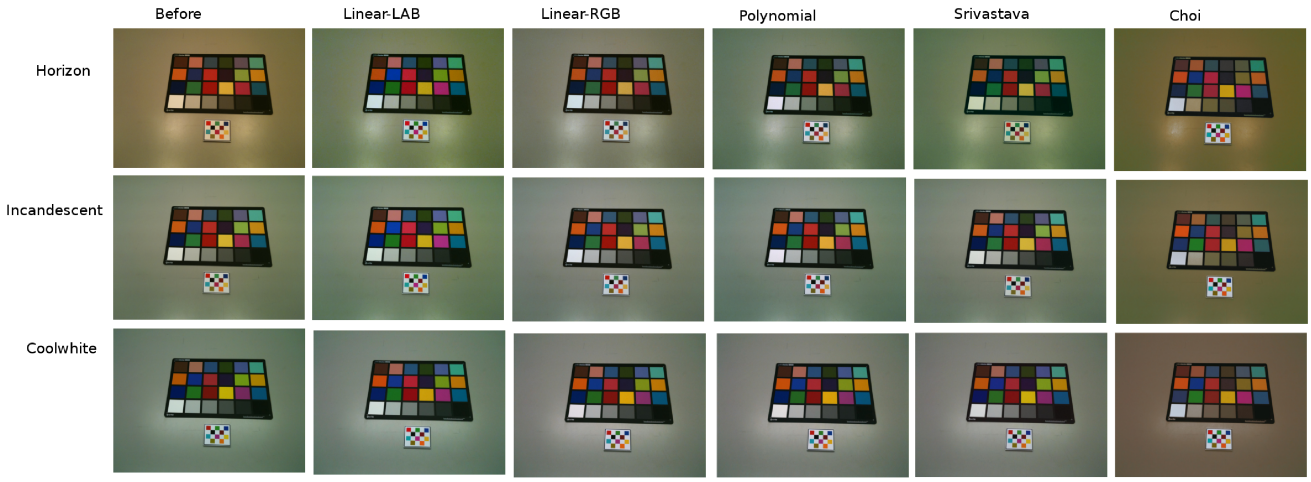

Figure 7. Comparison of the Five Color Correction Methods

lighting conditions. In the future, we can improve our methods by finding the gamma for each specific color channel and specific device and by exploring other factors(e.g. the reflectance properties of the object or the spectral sampling properties of the capturing device) that affect the color appearance model. We can also test our methods under more illumination conditions.

REFERENCES

1. M. B. E. Livingstone, P. J. Robson, and J. M. W. Wallace, "Issues in dietary intake assessment of children and adolescents," *British Journal of Nutrition*, vol. 92, pp. S213–S222, 2004.
2. M. U. Waling and C. L. Larsson, "Energy intake of swedish overweight and obese children is underestimated using a diet history interview," *Journal of Nutrition*, vol. 139, no. 3, pp. 522–527, March 2009.
3. C. J. Boushey, D. A. Kerr, J. Wright, K. D. Lutes, D. S. Ebert, and E. J. Delp, "Use of technology in children's dietary assessment," *European Journal of Clinical Nutrition*, vol. 63, pp. S50–S57, 2009.
4. B. Six, T. Schap, F. Zhu, A. Mariappan, M. Bosch, E. Delp, D. Ebert, D. Kerr, and C. Boushey, "Evidence-based development of a mobile telephone food record," *Journal of American Dietetic Association*, vol. 110, pp. 74–79, January 2010.
5. F. Zhu, M. Bosch, I. Woo, S. Kim, C. J. Boushey, D. S. Ebert, and E. J. Delp, "The use of mobile devices in aiding dietary assessment and evaluation," *IEEE Journal of Selected Topics in Signal Processing*, vol. 4, no. 4, pp. 756–766, August 2010.
6. I. Woo, K. Otsmo, S. Kim, D. S. Ebert, E. J. Delp, and C. J. Boushey, "Automatic portion estimation and visual refinement in mobile dietary assessment," *Proceedings of the IS&T/SPIE Conference on Computational Imaging VIII*, vol. 7533, San Jose, CA, January 2010, p. 75330O.

7. J. Chae, I. Woo, S. Kim, R. Maciejewski, F. Zhu, E. J. Delp, C. J. Boushey, and D. S. Ebert, "Volume estimation using food specific shape templates in mobile image-based dietary assessment," *Proceedings of the IS&T/SPIE Conference on Computational Imaging IX*, vol. 7873, January 2011, p. 78730K.
8. "USDA food and nutrient database for dietary studies, 1.0," Beltsville, MD: Agricultural Research Service, Food Surveys Research Group, 2004.
9. T. Schap, B. Six, E. Delp, D. Ebert, D. Kerr, and C. Boushey, "Adolescents in the united states can identify familiar foods at the time of consumption and when prompted with an image 14 h postprandial, but poorly estimate portions," *Public Health Nutrition*, vol. 1, no. 1, pp. 1–8, 2011.
10. M. Puri, Z. Zhu, Q. Yu, A. Divakaran, and H. Sawhney, "Recognition and volume estimation of food intake using a mobile device," *Proceedings of Workshop on Applications of Computer Vision (WACV)*, Piscataway, NJ, USA, December 2009, pp. 1–8.
11. G. Sharma, *Digital Color Imaging Handbook*. Boca Raton, Florida: CRC Press, 2002.
12. K. E. A. van de Sande, T. Gevers, and C. G. M. Snoek, "Evaluating color descriptors for object and scene recognition," *IEEE Transactions on Pattern Analysis and Machine Intelligence*, vol. 32, no. 9, pp. 1582–1596, September 2010.
13. K. Van De Sande, T. Gevers, and C. Snoek, "Evaluating color descriptors for object and scene recognition," *IEEE Transactions on Pattern Analysis and Machine Intelligence*, vol. 32, no. 9, pp. 1582–1596, September 2010.
14. F. Mindru, T. Tuytelaars, L. Van Gool, and T. Moons, "Moment invariants for recognition under changing viewpoint and illumination," *Computer Vision and Image Understanding*, vol. 94, no. 1-3, pp. 3–27, April/May/June 2004.
15. E. Reinhard, M. Adhikhmin, B. Gooch, and P. Shirley, "Color transfer between images," *IEEE Computer Graphics and Applications*, vol. 21, no. 5, pp. 34–41, September/October 2001.
16. G. Finlayson, S. Hordley, and P. Hubel, "Color by correlation: A simple, unifying framework for color constancy," *IEEE Transactions on Pattern Analysis and Machine Intelligence*, vol. 23, no. 11, pp. 1209–1221, November 2001.
17. H. Siddiqui and C. Bouman, "Hierarchical color correction for camera cell phone images," *IEEE Transactions on Image Processing*, vol. 17, no. 11, pp. 2138–2155, November 2008.
18. K. Barnard, V. Cardei, and B. Funt, "A comparison of computational color constancy algorithms. i: Methodology and experiments with synthesized data," *IEEE Transactions on Image Processing*, vol. 11, no. 9, pp. 972–984, September 2002.
19. Y. Choi, Y. Lee, and W. Cho, "Color correction for object identification from images with different color illumination," *Proceedings of the 2009 Fifth International Joint Conference on INC, IMS and IDC*, Piscataway, NJ, USA, August 2009, pp. 1598–1603.
20. S. Srivastava, E. Delp, T. Ha, and J. Allebach, "Color management using optimal three-dimensional look-up tables," *Journal of Imaging Science and Technology*, vol. 54, p. 030402, May-June 2010.
21. C. Xu, N. Khanna, C. Boushey, and E. Delp, "Low complexity image quality measures for dietary assessment using mobile devices," *Proceedings of the IEEE International Symposium on Multimedia*, Dana Point, CA, USA, December 2011.
22. J. McCann, "Color spaces for color-gamut mapping," *Journal of Electronic Imaging*, vol. 8, pp. 354–364, October 1999.
23. J. von Kries, "Chromatic adaptation," *Festschrift der Albrecht-Ludwigs-Universit*, pp. 145–158, 1902.
24. G. D. Finlayson and S. Susstrunk, "Performance of a chromatic adaptation transform based on spectral sharpening," *Proceedings of the IS&T/SID Color Imaging Conference*, Scottsdale, AZ, United states, November 2000, pp. 49–55.
25. R. W. G. Hunt, *The Reproduction of Color*. Hoboken, New Jersey: Wiley, 2004.
26. M. D. Fairchild, *Color Appearance Models*. Chichester, UK: Wiley, 2005.
27. M. Stokes, M. Anderson, S. Chandrasekar, and R. Motta, "A standard default color space for the internet-srgb," *Microsoft and Hewlett-Packard Joint Report*, 1996.
28. G. Johnson and M. Fairchild, "Visual psychophysics and color appearance," *Digital color imaging handbook, CRC Press*, pp. 115–172, 2003.
29. D. Pascale, "Rgb coordinates of the macbeth color checker," *Montreal, Quebec, Canada, The BabelColor Company. Updated*, vol. 1, 2006.